

ORIGINAL ARTICLE

The epsilon toxin from *Clostridium perfringens* stimulates calcium-activated chloride channels, generating extracellular vesicles in *Xenopus* oocytes

Mercè Cases^{1,2,3}  | Jonatan Dorca-Arévalo^{1,2,3}  | Marta Blanch^{1,2}  | Sergi Rodil¹  |
 Beatrice Terni^{1,2,3}  | Mireia Martín-Satué¹  | Artur Llobet^{1,2,3}  | Juan Blasi^{1,2,3}  |
 Carles Solsona^{1,2,3} 

¹Department of Pathology and Experimental Therapeutics, Faculty of Medicine and Health Sciences—Campus Bellvitge, University of Barcelona, Barcelona, Spain

²Laboratory of Molecular and Cellular Neurobiology, Bellvitge Biomedical Research Institute (IDIBELL), Hospitalet de Llobregat, Spain

³Institute of Neuroscience, University of Barcelona, Barcelona, Spain

Correspondence

Carles Solsona and Juan Blasi, Department of Pathology and Experimental Therapeutics, Faculty of Medicine and Health Sciences—Campus Bellvitge, University of Barcelona, Barcelona 08907, Spain.
 Email: blasi@ub.edu and solsona@ub.edu

Present address

Mercè Cases, Patvocates GmbH, Munich, Germany

Funding information

Centres de Recerca de Catalunya, Grant/Award Number: SGR: 2021 SGR 01075; Grant/Award Number: MCIN/

Abstract

The epsilon toxin (Etx) from *Clostridium perfringens* has been identified as a potential trigger of multiple sclerosis, functioning as a pore-forming toxin that selectively targets cells expressing the plasma membrane (PM) myelin and lymphocyte protein (MAL). Previously, we observed that Etx induces the release of intracellular ATP in sensitive cell lines. Here, we aimed to re-examine the mechanism of action of the toxin and investigate the connection between pore formation and ATP release. We examined the impact of Etx on *Xenopus laevis* oocytes expressing human MAL. Extracellular ATP was assessed using the luciferin-luciferase reaction. Activation of calcium-activated chloride channels (CaCCs) and a decrease in the PM surface were recorded using the two-electrode voltage-clamp technique. To evaluate intracellular Ca²⁺ levels and scramblase activity, fluorescent dyes were employed. Extracellular vesicles were imaged using light and electron microscopy, while toxin oligomers were identified through western blots. Etx triggered intracellular Ca²⁺ mobilization in the *Xenopus* oocytes expressing hMAL, leading to the activation of CaCCs, ATP release, and a reduction in PM capacitance. The toxin induced the activation of scramblase and, thus, translocated phospholipids from the inner to the outer leaflet of the PM, exposing phosphatidylserine outside in *Xenopus* oocytes and in an Etx-sensitive cell line. Moreover, Etx caused the formation of extracellular vesicles, not derived from

Abbreviations: A.U, Arbitrary Units of luminescence or gray intensity of electron negative stained micrographs; CaCC, Calcium-activated chloride channels; cRNA, complementary RNA; EVs, Extracellular vesicles; EGTA, Ethylene glycol-bis (2-aminoethylether)-N,N,N',N'-tetraacetic acid; ER-PM junctions, Endoplasmic Reticulum-Plasma Membrane Junctions; Etx, Epsilon toxin from *Clostridium perfringens*; GPCRs, G-protein-coupled receptors; hMAL, human Myelin and Lymphocyte protein; IP3, Inositol 1,4,5-trisphosphate; MAL, Myelin and Lymphocyte protein; MARVEL, MAL and related proteins for vesicle trafficking and membrane link; MONNA, N-((4-methoxy)-2-naphthyl)-5-nitroanthranilic acid; pEtx, Prototoxin of Epsilon toxin from *Clostridium perfringens*; PFTs, Pore-forming bacterial toxins; PM, Plasma membrane; PS, Phosphatidylserine; pSIVA, Polarity-sensitive indicator of viability and apoptosis; SEM, Standard error of the mean; ST, Staurosporine; TeNT-LC, The light chain of tetanus neurotoxin; TMEM16A, Transmembrane protein 16A; TMEM16F, Transmembrane protein 16F; hTMEM16F, Transmembrane protein 16F; WT, Wild type *Xenopus* oocytes; xMAL, *Xenopus* Myelin and Lymphocyte protein; α -xMAL, Antisense oligonucleotide for xMAL; α -xTMEM16A, Antisense nucleotide against the endogenous CaCC.

Mercè Cases and Jonatan Dorca-Arévalo contributed equally to this work.

This is an open access article under the terms of the [Creative Commons Attribution-NonCommercial](https://creativecommons.org/licenses/by-nc/4.0/) License, which permits use, distribution and reproduction in any medium, provided the original work is properly cited and is not used for commercial purposes.

© 2024 The Author(s). *Pharmacology Research & Perspectives* published by British Pharmacological Society and American Society for Pharmacology and Experimental Therapeutics and John Wiley & Sons Ltd.

AEI/10.13039/501100011033, PID2021-126677NB-I00 and SAF2017-85818-R; European Regional Development Fund

apoptotic bodies, through PM fission. These vesicles carried toxin heptamers and doughnut-like structures in the nanometer size range. In conclusion, ATP release was not directly attributed to the formation of pores in the PM, but to scramblase activity and the formation of extracellular vesicles.

KEYWORDS

calcium-activated chloride channels, epsilon toxin, extracellular vesicles, pore-forming toxins, scramblase, TMEM16A, *Xenopus laevis* oocytes

1 | INTRODUCTION

Pore-forming bacterial toxins (PFTs) are remarkable proteins that are secreted as soluble hydrophilic monomers. Upon activation, they assemble into oligomers that are then inserted within the plasma membrane (PM).^{1,2} The epsilon toxin (Etx), a PFT produced by *Clostridium perfringens* types B and D, is thought to exert its cytotoxic effect by creating ion-conducting pores in planar lipid bilayers. The crystal structure of the soluble monomer of Etx has been revealed through x-ray crystallography,³ while cryo-electron microscopy has shown that its heptameric structure consists of a double β -barrel pore, which has a large internal lumen measuring 2.4 nm in diameter.⁴

The effect of Etx on cellular processes has been gaining increasing attention, particularly regarding its potential involvement in the development and progression of multiple sclerosis, a severe demyelinating disease associated with immune system dysfunction.⁵⁻⁷ Etx has a selective cellular action due to its specific interaction with its putative receptor, the myelin and lymphocyte protein (MAL). The pivotal study demonstrating the requirement of MAL for the cytotoxic and lethal activity of Etx⁸ has been supported by subsequent investigations,⁹⁻¹² making MAL the most widely accepted receptor candidate. MAL is a 17-kDa protein with four transmembrane domains and is highly expressed in T lymphocytes, myelin, and polarized epithelial cells. Notably, it has been shown that only cells expressing MAL are sensitive to Etx.^{9,13-15}

Etx stimulates the release of ATP in cells that express MAL,^{9,13,16-18} suggesting an Etx-mediated direct communication between the cytosol and the extracellular media. This ATP release is believed to occur through channels formed by the Etx oligomers. In contrast to cell culture, the experimental model of *Xenopus* oocytes offers a unique opportunity to record the release of ATP from a single cell¹⁹ and is electrically accessible to detect the presence of toxin pores at their PM.

Cellular swelling and the formation of membrane blebs are characteristic features observed in cells impacted by PFTs.²⁰⁻²² Similar results have been documented in cells exposed to Etx.²³⁻²⁶ However, the specific molecular mechanisms underlying these changes in membrane reorganization remain unknown. In this study, we aimed to investigate the mechanisms underlying Etx-dependent ATP release and the formation of extracellular vesicles (EVs) through the

involvement of **scramblases**, a group of enzymes that facilitate the exchange of phospholipids between the two leaflets of the membrane.²⁷ Scramblases are also known to contribute to membrane curvature and the formation of EVs.²⁷ Interestingly, scramblases belong to the same family as **calcium-activated chloride channels (CaCCs)**, which are naturally expressed in the PM of *Xenopus laevis* oocytes. Therefore, we examined the impact of Etx on *Xenopus laevis* oocytes expressing human MAL (hMAL), in combination with the MOLT-4 cell line, to elucidate the role of CaCCs and scramblases in Etx-mediated actions.

2 | MATERIALS AND METHODS

The materials and methods used are thoroughly explained in the S1 section. In summary, the synthesis and activation of pEtx were performed as previously described.^{9,17} *Xenopus laevis* specimens were handled in accordance with the guidelines approved by the local Catalan Government (reference 192/16, Animal Welfare Committee of the University of Barcelona). *Xenopus laevis* oocytes were defolliculated using Liberase™ and subsequently injected with cRNA encoding the membrane proteins of interest. The hMAL gene was cloned from cDNA.⁹ The silencing of the endogenous membrane proteins xMAL and xTMEM16A was achieved through the injection of antisense oligonucleotides.

Extracellular ATP levels were continuously measured using the D-luciferin and luciferase reaction. Two-electrode voltage-clamp was utilized to record membrane currents and capacitance. Intracellular **calcium** levels and scramblase activity were observed using Calbryte™ 520 and pSIVA™-IANBD on a confocal microscope. The generation of EVs, retrieved via centrifugation from the oocyte treatment medium, was observed through phase-contrast microscopy and analyzed with electron microscopy or conventional immunoblotting.

Scramblase activity was also assessed in the MOLT4 cell line⁹ using confocal microscopy and flow cytometry. For recording ATP release and the voltage-clamp experiments, we used two recording solutions: Frog Ringer (FR), which contained 115 mM NaCl, 2 mM KCl, 1.8 mM CaCl₂, 1 mM MgCl₂, and 10 mM HEPES (pH 7.6, osmolarity 220 mOsm), and Mg-FR with 1 mM EGTA (MgFR-1 mM EGTA or low Ca²⁺), which contained 115 mM NaCl, 2 mM KCl, 1 mM MgCl₂,

0.1mM CaCl_2 , 1mM EGTA, and 10mM HEPES (pH7.6, osmolarity 220mOsm, and an estimated $[\text{Ca}^{2+}]$ of 3nM).

The data and statistical analysis adhered to the recommendations of the *British Journal of Pharmacology* regarding the experimental design and analysis in pharmacology.²⁸

2.1 | Nomenclature of targets and ligands

Key protein targets and ligands in this article are hyperlinked to corresponding entries in <http://www.guidetopharmacology.org>, the common portal for data from the IUPHAR/BPS Guide to PHARMACOLOGY,²⁹ and are permanently archived in the Concise Guide to PHARMACOLOGY 2019/20.^(30,31)

3 | RESULTS

3.1 | Oocyte PM permeability

ATP release was recorded in single *Xenopus* oocytes using the D-luciferin-luciferase luminescence reaction. Oocytes injected with hMAL cRNA (hMAL oocytes) released ATP in the presence of Etx, whereas the control non-injected oocytes (WT) were insensitive to Etx and did not release ATP. We did not observe any release of ATP from hMAL oocytes when the prototoxin (pEtx) (the toxin precursor with much less activity) was used instead of the active Etx (Figure 1A). We explored two pathways of ATP release: through Etx pores in the PM or by the exocytosis of secretory granules.

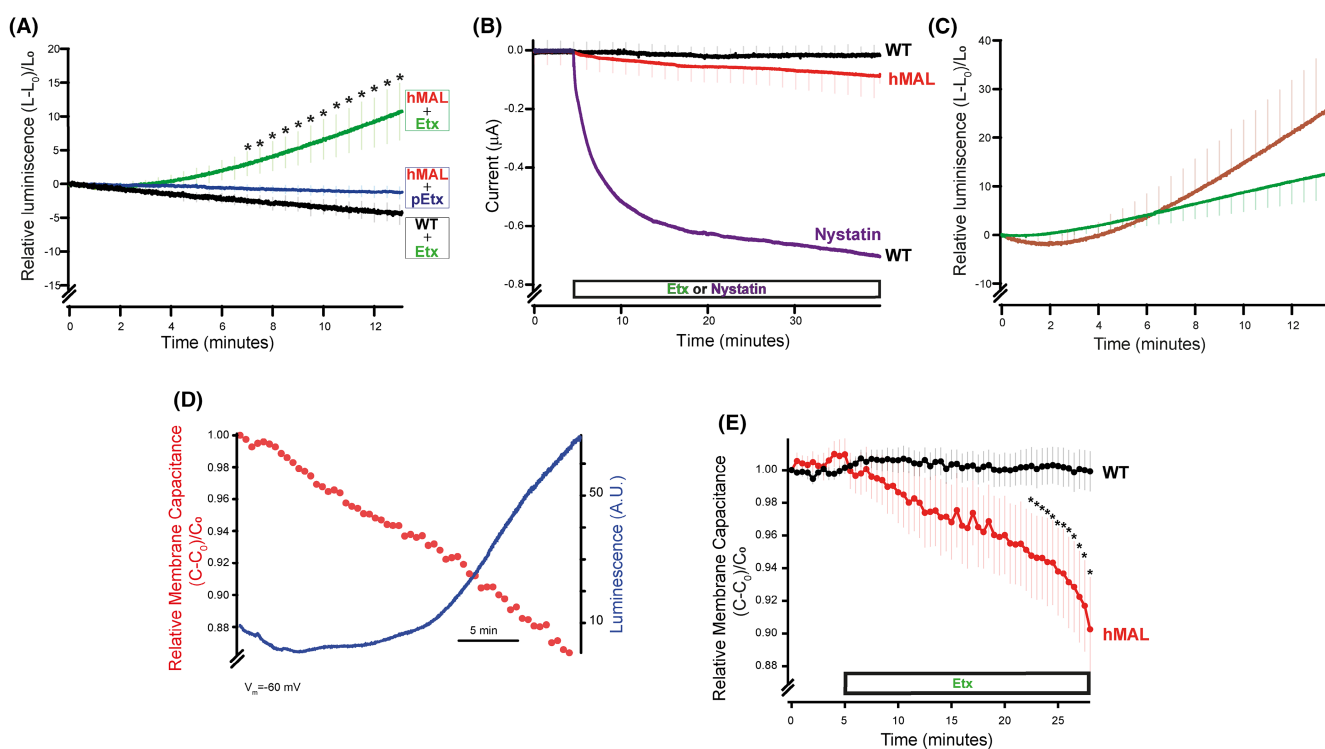


FIGURE 1 EtX induced ATP release from individual *Xenopus laevis* oocytes. (A) ATP release from single oocytes. EtX was added at time 0. The green trace is the mean of the relative increase in light due to the release of ATP from oocytes expressing hMAL. Solution, (FR) with CaCl_2 and EtX 300nM ($N=10$). Black trace, wild-type (WT) oocytes in the same condition ($N=10$). Blue trace, oocytes expressing hMAL treated with 300nM of the prototoxin, pEtX ($N=5$). Vertical bars represent \pm SEM at the indicated times. Note that in WT treated with EtX and in hMAL oocytes treated with prototoxin, the negative relative luminescence values were due to the spontaneous decline in the initial light emitted by the luciferin-luciferase reaction, indicating that no ATP was released. (B) EtX (300nM) induced currents. Red trace, hMAL expressing oocytes, $N=12$. Black trace, WT oocytes, $N=10$. The membrane potential fixed at -40mV . Traces are the mean of the traces obtained from individual oocytes. Vertical bars represent \pm SEM at the indicated times; for clarity, only half of the bars are shown. Violet trace, a known pore-forming compound (nystatin, $40\mu\text{M}$). A single record showing an increment in the inward current. The solid black box represents the presence of nystatin or EtX in the medium. (C) The light chain of tetanus neurotoxin (TeNT-LC) was used to test whether ATP release was due to the exocytosis of cortical granules of the oocytes. In the presence of EtX (300nM). Brown trace, ATP release in oocytes expressing hMAL and injected with TeNT-LC (brown trace, T-LC inj, ($N=10$ oocytes). Green trace, oocytes expressing hMAL not injected with TeNT-LC, $N=24$. As in (A), EtX was added at time 0. (D) Plot of simultaneous recording of the relative membrane capacitance (red dots) and ATP release/ luminescence (blue trace) of an individual hMAL-expressing oocyte. Note that while luminescence increases PM capacitance decreases. EtX, 300nM. Luminescence is expressed in arbitrary units (A.U.). As in (A) and (C), EtX was added at time 0. (E) Changes in the relative membrane capacitance. Red line, hMAL oocytes, $N=8$. Black line, WT oocytes, $N=11$. Membrane potential was clamped at -60mV . Vertical bars represent \pm SEM at the indicated times. The solid black bar indicates the presence of EtX (300nM) in the medium. Statistical significance (*) $p < .05$.

In contrast to the effect of other PFTs,³² Etx induced only a negligible increase in the PM conductance of hMAL oocytes clamped at -40 mV (Figure 1B), suggesting the absence of pore formation by Etx. However, nystatin, a well-known pore-forming agent used as a positive control, induced a current of up to $0.7 \mu\text{A}$ (Figure 1B).

Secretory granules may undergo exocytosis by constitutive or regulated pathways. We explored the possibility that the regulated exocytosis of endogenous secretory granules of oocytes releases ATP by pre-injecting the light chain of the tetanus neurotoxin (TeNT-LC), which blocks exocytosis by cleaving synaptobrevin in *Xenopus* oocytes.³³ However, this strategy did not impair Etx-induced ATP release (Figure 1C, S1A). It should be noted that the proteolytic activity of the injected TeNT-LC had been previously checked in rat brain synaptosomes (Figure S1B). To test a hypothetical SNARE-independent pathway of exocytosis, we also measured PM capacitance on the basis that the exocytosis of endogenous secretory granules should cause an increase in the cell PM capacitance; however, contrary to the expected result, we observed a slight decrease (Figure 1D,E) that was absent from the WT oocytes treated with Etx.

3.2 | Intracellular Ca^{2+} concentration

Although ATP was not released via secretory granule exocytosis, which requires an increase in intracellular $[\text{Ca}^{2+}]$, we wanted to check the dependence of Etx-induced ATP release on this cation. To test this, we first evaluated the effect of the intracellular injection of the Ca^{2+} chelating agent EGTA, which prevented Etx-induced ATP release (Figure 2A, Figure S2A). Conversely, an extracellular solution containing EGTA with an estimated final concentration of 3 nM Ca^{2+} sustained the Etx-induced ATP release (Figure 2A, Figure S2A), suggesting that the ATP release depends on intracellular Ca^{2+} mobilization. The increase in intracellular $[\text{Ca}^{2+}]$ induced by Etx was effectively monitored using the Ca^{2+} indicator Calbryte™ 520 (Figure 2B), with the Ca^{2+} ionophore A23187 as the control (Figure S2B).

3.3 | CaCC activation

To further explore the effect of the Etx-induced increase in intracellular $[\text{Ca}^{2+}]$, we measured CaCC activity in *Xenopus* oocytes. CaCCs are exquisite sensors of intracellular $[\text{Ca}^{2+}]$ that are activated by changes in intracellular $[\text{Ca}^{2+}]$ and voltage.^{34–36} Etx, but not pEtx, activated endogenous CaCCs (Figure 2C), increasing the currents obtained at $+90$ mV in both the hMAL and WT oocytes (Figure 2D, Figure S2C). In the hMAL oocytes, the increase was almost two-fold compared to that in the WT oocytes, with the maximal response observed at 20 min.

CaCC currents were larger in the hMAL oocytes than in the WT ones. This difference might be related to variations in the molecular structures of hMAL and the endogenous *Xenopus* MAL (xMAL), which both contain four transmembrane domains. A comparison of the sequences and the tertiary structure of both proteins showed their similarity, as presented in Figure S3A,B.

Injecting antisense oligonucleotide (α -xMAL) to prevent the translation of the xMAL mRNA strongly inhibited the Etx-dependent activation of CaCCs in the WT oocytes (Figure 3A).

As stated above, hMAL oocytes, but not WT oocytes, released ATP under the influence of Etx (Figure 1A). To confirm the role of CaCCs in ATP release in the hMAL oocytes and the activation of the ionic current by Etx, we used *N*-((4-methoxy)-2-naphthyl)-5-nitroanthranilic acid (MONNA), a potent and selective inhibitor of slow and fast components of the CaCC.³⁷ MONNA inhibited the Etx-activated CaCC currents in the hMAL oocytes (Figure 3B), but also strongly decreased Etx-induced ATP release (Figure 3C, Figure S4A). We ruled out a direct effect (at the concentration used) of MONNA on the luminescence reaction used to detect ATP. Moreover, the injection of the antisense nucleotide against endogenous CaCCs (α -xTMEM16A) decreased ATP release (Figure 3C, Figure S4A) and Etx-activated CaCC currents (Figure 3D). The reversal potentials of currents activated by Etx were in the expected range of the equilibrium potential of Cl^- . Although there was no significant difference between the hMAL and WT oocytes treated with the toxin, the reversal potential at time zero was significantly different to that at 20 min in both conditions (Figure S4B).

3.4 | Morphological changes at the oocyte surface

Morphological comparison of the oocyte surface by light interference microscopy before (Figure 4A) and after Etx incubation (Figure 4B) revealed the presence of small spherical structures moving and flickering in close contact with the PM (Movie S1). The observations of the oocyte surface (Movies S1 and S2) indicated vesicle budding and shedding from the PM as a result of the action of Etx (Figure 4C and Movies S1 and S2). By contrast, pEtx did not induce the massive release of EVs (Figure 4D–G).

Under the electron microscope, the outer surface of the oocytes was not smooth due to the presence of numerous microvilli on the cell PM. Figure S5 shows the cell surface structure of *Xenopus* oocytes. On the cytoplasmic side of the PM in the defolliculated oocytes, we found numerous expansions of the endoplasmic reticulum (ER) (Figure 5A–D) forming the so-called endoplasmic reticulum–plasma membrane (ER–PM) junctions.³⁸ Etx did not severely disorganise the distribution of the oocyte granules in the cortical zone, but did change the PM, causing a decrease in the number of microvilli and the appearance of complex spherical structures (Figure 5E–H).

3.5 | Scramblase activity

Phospholipid scrambling has been associated with the release of EVs.²⁷ Scramblases typically break the asymmetric distribution of phospholipids in cell membranes, moving PS from its usual location on the inner leaflet of PMs to the outer leaflet. This redistribution of PS to the external cell surface can be monitored with the fluorescent probe polarity-sensitive indicator of viability and apoptosis (pSIVA). In the hMAL oocytes, Etx induced a diffuse increase in the fluorescence of pSIVA,

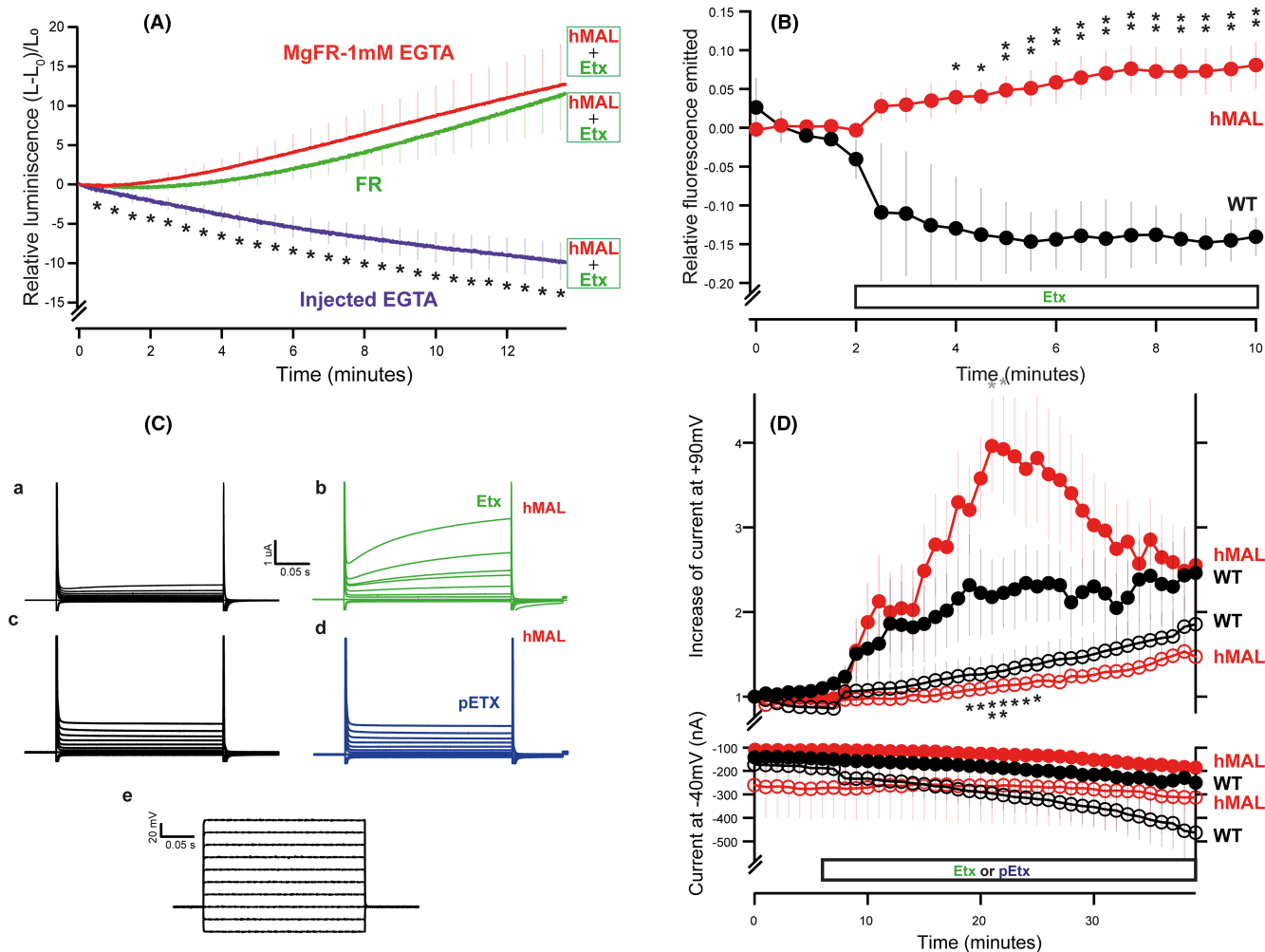


FIGURE 2 Intracellular Ca^{2+} is a key element for calcium-activated chloride channels. (A) ATP release from oocytes injected with hMAL RNA: Green trace, oocytes in FR (1 mM CaCl_2 and 1 mM MgCl_2 ; $N=10$); red trace, oocytes bathed in the MgFR 1 mM EGTA solution ($N=32$) with an estimated $[\text{Ca}^{2+}]$ of 3 nM. Dark blue trace, EGTA (3 μM) injected hMAL oocytes in the FR bathing solution, $N=13$. The negative relative luminescence values reflect the spontaneous decline in initial luminescence. Etx (300 nM) was added at time zero. (B) CalbryteTM 520 fluorescence emitted by oocytes. Red trace, hMAL oocytes, $N=5$. Black trace, WT oocytes, $N=3$. The horizontal solid black bar indicates the presence of Etx (300 nM) in the low Ca^{2+} recording solution (MgFR 1 mM EGTA). Because this fluorescent methodology does not measure the actual intracellular $[\text{Ca}^{2+}]$, we used a limited number of oocytes to reduce the number of animals utilized (only three). Significance: (*) $p < .05$; (**) $p < .01$. (C) Endogenous currents of voltage-dependent calcium-activated chloride channels (CaCC) activated by Etx in hMAL oocytes: (a) black traces, before and (b) green traces, 5 min after adding the toxin (300 nM). Notice that slow-onset currents at positive potentials; (c) black traces, recording before and (d) dark blue traces, 5 min after adding pEtx (300 nM); (e) stimulus protocol (oocyte clamped at -40 mV and square stimuli from -80 mV to $+100$ mV for 250 ms). (D) Time course of Etx-induced currents. *Upper panel*: Red filled circles, hMAL oocytes, $N=11$; black filled circles, WT oocytes, $N=14$. Each point corresponds to the current increase, at the indicated time, at the end of a pulse of $+90$ mV for 250 ms. Red empty circles and black empty circles, effect of pEtx on hMAL oocytes ($N=4$) and WT oocytes ($N=11$) respectively. *Lower panel*: Currents were stable at -40 mV in all conditions tested, as in the *upper panel*. Symbols mean same as the upper panel. The horizontal bar represents the addition of Etx or pEtx at 300 nM at the indicated time. In the upper panel, asterisks in gray correspond to differences between hMAL and WT oocytes treated with Etx, while the black asterisks and double asterisks correspond to the comparison between hMAL oocytes treated with Etx or pEtx. Significance: (*) $p < .05$; (**) $p < .01$.

with some bright spots (Figure S6A,B,E; in red), in contrast to that observed with pEtx (Figure S6C-E; in blue). This suggested the presence of Etx-induced scramblase activity. In the Etx-sensitive MOLT-4 cell line, Etx induced the extracellular exposure of PS, while pEtx did not (Figure S6F,G, and Movies S3 and S4). This effect was corroborated by flow cytometry (Figure S7). The exposure of PS on the extracellular leaflet of the PM is a characteristic of cell apoptosis, a cell death process

that releases EVs as apoptotic bodies.³⁹ To determine whether Etx induces cell apoptosis, we analyzed cleaved caspase-3 in MOLT-4 cells. Etx did not activate caspase-3 during the 20 min of its action (Figure 6). As a positive control, MOLT-4 cells were incubated with staurosporine (ST) overnight,⁴⁰ which resulted in the cleavage of caspase-3. Even after the prolonged overnight incubation with Etx, the activation of caspase-3, which would be indicative of apoptosis, was not observed (Figure 6).

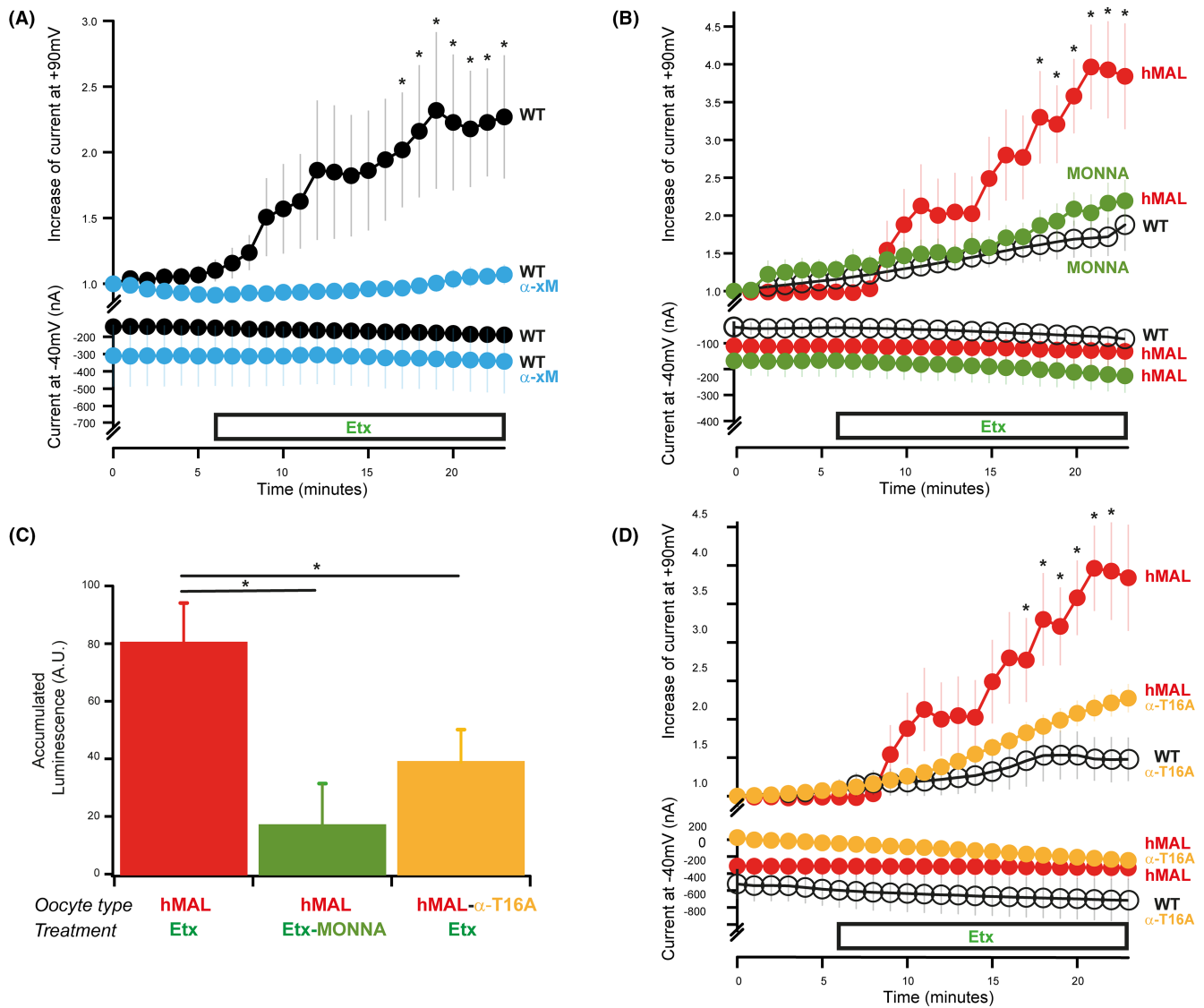


FIGURE 3 Etx targets TMEM16A. (A) MAL- and Etx-dependent activation currents. *Upper panel*, currents at the end of a pulse of +90mV for 250ms. Black circles, WT oocytes, data from [Figure 2D](#) ($N = 14$). Sky blue circles represent WT α -xM oocytes, corresponding to WT oocytes previously injected with the antisense oligonucleotide against endogenous *Xenopus* MAL (α -xMAL) ($N = 8$ oocytes). *Lower panel*, currents measured at -40mV. The horizontal bar represents the addition of Etx or pEtx at 300nM at the indicated time. Significance: (*) $p < .05$. (B) Effect of MONNA (10 μ M), a potent blocker of CaCC, on currents. *Upper panel*: Currents at +90mV. Red filled circles, hMAL-oocytes (data from [Figure 2D](#), $N = 11$). Green filled circles, MONNA in hMAL oocytes (gray trace; $N = 10$, (*) $p < .05$). Black empty circles, effect of MONNA on WT oocytes ($N = 10$). For clarity, Etx-activated currents in WT oocytes ([Figure 3A](#)) are not included. *Lower panel*: MONNA did not alter currents at -40mV. Symbols are the same as the upper panel. The horizontal bar represents the addition of Etx or pEtx at 300nM at the indicated time. Significance: (*) $p < .05$. (C) Etx-induced ATP release was dependent on MAL and TMEM16 protein expression. The release of ATP is represented by bars corresponding to the accumulated light of individual oocytes during the action of Etx. The ochre bar, labeled 'hMAL oocytes α -T16A-Etx,' indicates recordings made in hMAL oocytes preinjected with antisense oligonucleotides against endogenous *Xenopus* oocyte CaCCs (α -xTMEM16A). The sample sizes were: hMAL oocytes with Etx, $N = 19$; hMAL oocytes with MONNA and Etx, $N = 6$; and hMAL oocytes with α -xT16 and Etx, $N = 14$. Significance: (*) $p < .05$. (D) Analysis of Etx-dependent activation currents in hMAL oocytes injected with α -xTMEM16A oligonucleotides. *Upper panel*: +90mV evoked currents. hMAL oocytes (data from [Figure 2D](#), $N = 11$). Ochre filled circles, hMAL oocytes injected with oligonucleotide antisense α -xTMEM16A, labeled as hMAL α -T16A, $N = 14$. Black empty circles, WT oocytes injected with α -xTMEM16A, labeled as WT α -T16A ($N = 10$). As in panel 3B, Etx-activated currents in WT oocytes are not shown. *Lower panel*: The antisense oligonucleotide did not modify currents at the holding potential of -40mV. The horizontal bar represents the addition of Etx or pEtx at 300nM at the indicated time. Significance: (*) $p < .05$.

The molecular structure of CaCC was resolved and identified as TMEM16A, one of 10 TMEM16 membrane proteins classified from A to K.²⁷ The TMEM16A protein and its mRNA have been identified

in *Xenopus laevis* oocytes⁴¹ and the TMEM16F mRNA has also been detected in *Xenopus* oocytes.^{42,43} While CaCCs are anionic channels, TMEM16F has been identified as a cation channel⁽⁴⁴⁾ with scramblase

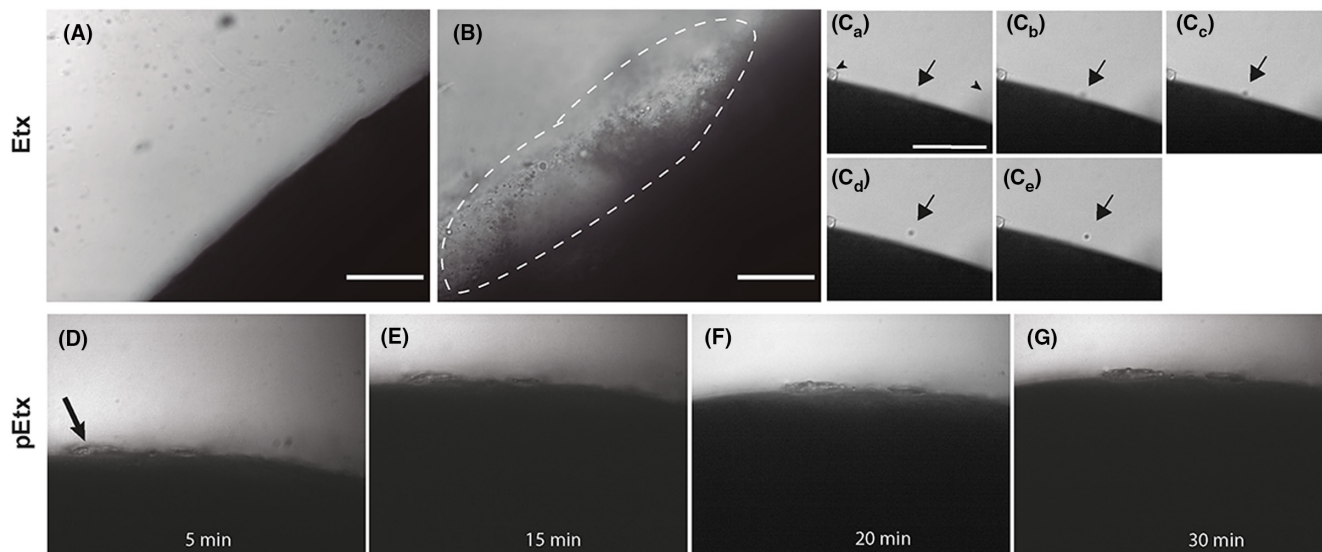


FIGURE 4 Generation of EVs in Etx-treated hMAL oocytes. (A) Interference light microscopy image of the oocyte surface before adding the toxin. The dark zone corresponds to the oocyte as a non-transparent body. The interface between the oocyte surface and the medium was diaphanous. (B) Image of this interface after 30 min exposure to Etx. In the area delimited with a white discontinuous line, the focal plane was adjusted to reveal vesicles after the addition of toxin. Vesicle-like structures accumulated around the oocyte with the appearance of bright or dark spheres of different diameters (scale bar for I and J: 100 μ m, [Movie S1](#)). These observations were made in oocytes from six independent experiments. (C) Image sequence (C_a–C_e) of the formation and excision of an EV taken from [Movie S2](#). The black surface corresponds to a delimited area of an oocyte. The black arrows point to the vesicle being excised from the oocyte. Images were taken every 30 s. In (C_a), the vesicle appears fuzzy and out of focus, but in contact with the PM; in (C_b), (C_c) and (C_d), it is moving towards the plane of focus; in (C_d) and (C_e) appears clearly separated from the PM; in (C_e), it is nearly in the plane of focus. Arrowheads in (C_a) point to an attached EV and the shadow of another vesicle (scale bar: 100 μ m). (D–G) Effect of pEtx. The interface between the oocyte's surface and the surrounding medium is transparent. Notably, remnants of the follicular layer are visible on the oocyte's surface, indicated by the arrow. The focal plane was periodically adjusted to capture these remnants. Our observations from four distinct experiments reveal that the presence of EVs remained minimal within a 30-min period when pEtx was administered at a concentration of 300 nM. Magnification is the same as that of (B).

activity that permits lipid exchange between the membrane leaflets without the expenditure of metabolic energy. To explore the possible role of TMEM16F (with its inherent scramblase activity) in Etx-induced ATP release, human TMEM16F was co-overexpressed with hMAL in *Xenopus* oocytes. This co-overexpression, which is required because endogenous xTEM16F is poorly expressed in the PM,⁴³ resulted in a decrease in Etx-induced ATP release ([Figure S8A](#)). In this context, the apparent affinity of Ca²⁺ for TMEM16F was lower than that for TMEM16A.⁴⁵ To overcome this, we increased Ca²⁺ entry by using the Ca²⁺ ionophore A23187 in a medium containing 1 mM CaCl₂, which activated CaCC currents in the WT oocytes ([Figure S8B,C](#)). Using this approach, ATP release was not observed in the WT oocytes, but it was detected in the oocytes expressing hTMEM16F (human TMEM16F) in the presence of A23187 and a very high (10 mM) extracellular concentration of CaCl₂ ([Figure S8D,E](#)), with ATP release also lower than that in the hMAL oocytes treated with Etx.

3.6 | EVs and Etx oligomers

The EVs derived from the Etx-treated hMAL oocytes were concentrated by centrifugation and subjected to western blot analysis. The supernatant was free of any label. The membranous fraction displayed two bands. The stronger band with the lower molecular

weight corresponded to Etx monomers, while the other band of roughly 213 kDa corresponded to Etx heptamers ([Figure 7A](#)). Under electron microscopy with negative staining (a different technique to that used in [Figure 5A–H](#)), we observed the ultrastructure of the EVs. At a higher resolution, doughnut-like structures were observed that measured 22.8 nm in diameter, with an inner barrel measuring 8.5 nm ([Figure 7B–G](#)).

4 | DISCUSSION

We report several new key findings regarding the effects of Etx on *Xenopus* oocytes. Etx mobilizes intracellular calcium, activates CaCCs, exposes PS on the PM, promotes EV formation, does not form membrane pores directly in the PM, and triggers ATP release. Additionally, EVs contain Etx oligomers and show structures resembling membrane pores. We aim to address and unify these observations in our Discussion.

Our initial hypothesis was that Etx pores can account for ATP release based on a previous report showing that Etx forms pores in lipid bilayers⁴⁶ as well as on a study revealing the cryo-electron microscopic structure of Etx pores assembled on membranes.⁴ The pores have a large conductance (500 pS)⁴⁶ and an inner diameter of 2.4 nm⁴ and should permit the passage of ATP molecules, given

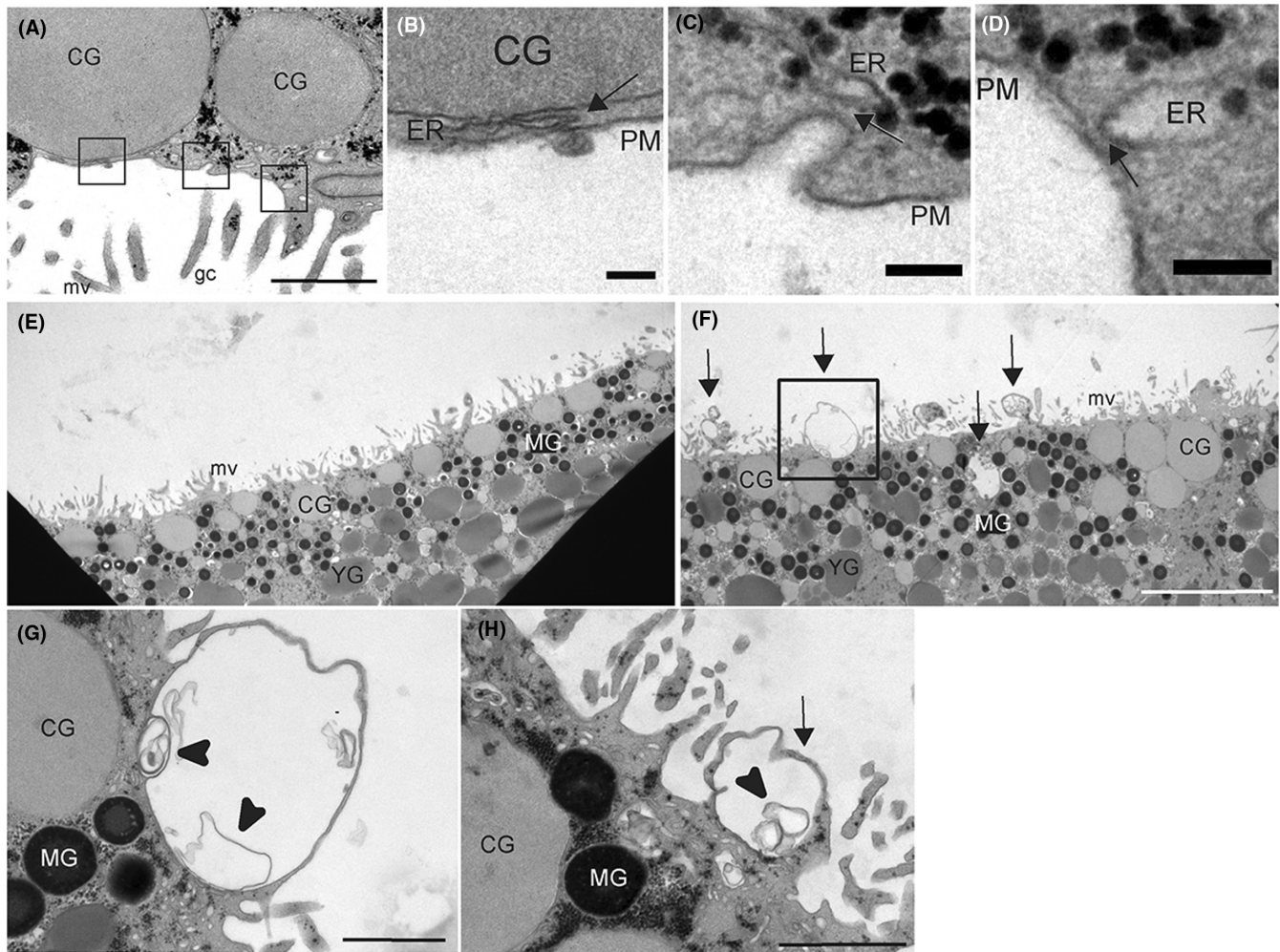


FIGURE 5 Ultrastructural changes of the PM induced by Etx. (A) Electron micrograph of a WT oocyte segment containing cytoplasmic cortical granules (GC) and PM. Note the highly undulated PM with numerous microvilli (mv) covered with a glycocalyx (gc). Endoplasmic reticulum cisternae (ER) were abundant near the PM (scale bar: 1 μ m). (B–D) correspond to higher magnifications of the square's insights from (A). The arrow shows the ER in close contact with the PM (i.e., ER–PM junctions). Scale bar for A=0.2 μ m; for (B–D), scale bar=0.1 μ m). (E) The surface and the PM of a defolliculated WT oocyte. Note the microvilli (mv) of the PM, the CG close to the PM, the smaller dark granules containing melanin (MG) and the yolk granules (YG) in the deepest part of the micrograph. The black shadow corresponds to the copper grid. (F–H) Etx-induced EVs generation in hMAL oocytes. (F) Effect of 30 min' exposure of hMAL oocyte to Etx (300 nM). While granules showed no apparent change, the PM showed sophisticated changes, especially the presence of spherical structures (arrows) (scale bar for E and F: 10 μ m). (G) shows the content of the inset from (F), where a spherical structure is delimited by a double PM separated by a very thin portion of cytoplasm containing internal membranes (arrowheads). (H) Another example of a spherical structure (arrow) from a different hMAL oocyte with slightly different organization, also showing internal membranous structures (arrowheads) (scale bar for G and H: 1 μ m). Images were obtained from two independent experiments.

their diameter of 0.7 nm.⁴⁷ However, our electrophysiological experiments with Etx-treated hMAL oocytes showed that Etx did not significantly increase the PM conductance, which is in contrast to the action of another pore-forming toxin (PFT) (Cry toxin) in *Xenopus* oocytes.³² Consequently, at least in the case of *Xenopus* oocytes, ATP is released through alternative pathways. Further details are provided in [Supplementary Comment 1](#).

We investigated whether the exocytosis of endogenous granules in *Xenopus* oocytes could be an alternative mechanism for ATP release. Our findings indicate that Etx-induced ATP release is dependent on intracellular $[Ca^{2+}]$, which supports the exocytosis of secretory granules. However, LC-TeNT, an inhibitor of granule

exocytosis in *Xenopus* oocytes,³³ did not inhibit Etx-induced ATP release. Typically, secretory granule exocytosis increases membrane capacitance due to the addition of the membranes of the secretory granules. By contrast, we observed a reduction in membrane capacitance. Experiments with simultaneous luminescence and current recordings revealed a delayed ATP release compared to the membrane capacitance decrease, supporting the conclusion that ATP release is independent of exocytosis.

The decrease in membrane capacitance coincided with the presence of EVs surrounding the oocyte surface, suggesting that the formation of these vesicles accounts for the reduction in the PM surface area. EVs are recognized for their roles in cell physiology^{48–50} and

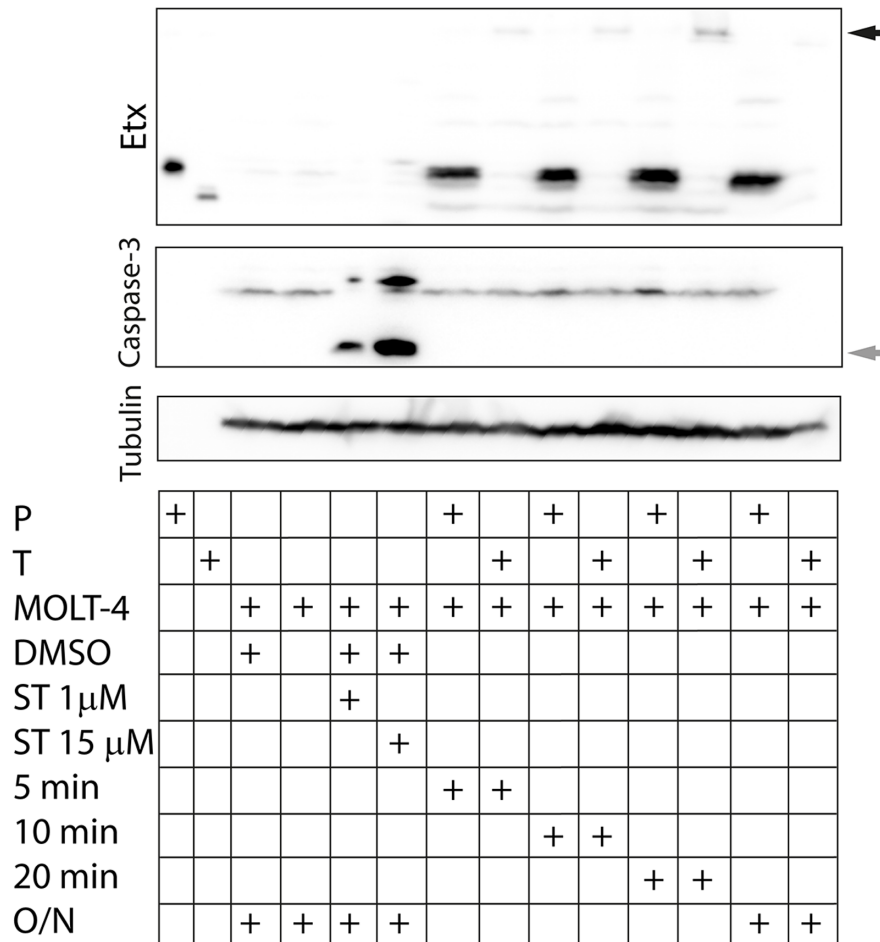


FIGURE 6 Testing the apoptotic effect of EtX. MOLT-4 cells were treated with pEtX, (P) or EtX (T) for 5, 10, and 20min, as well as overnight (O/N). The shorter times (5, 10, and 20min) correspond to periods preceding the formation of membrane blebs. To determine whether EVs induced by EtX are apoptotic bodies due to early apoptosis activation, the cleavage of caspase-3 was assayed. In the upper panel, EtX is detected both as a monomer and as oligomers, with oligomer mobility indicated by a black arrow. Oligomers, which become more evident after 20min of incubation, serve as a fingerprint of EtX action. In the middle panel, no cleaved caspase-3 bands were observed except in cells treated overnight (O/N) with staurosporine (ST) at two concentrations used. The gray arrow indicates the cleaved caspase-3 band. In contrast, no active caspase-3 was detected in cells incubated overnight with EtX. Note that the vehicle in which staurosporine was diluted (dimethyl sulfoxide, DMSO) did not activate caspase-3 either. In the lower panel, tubulin was detected as a loading control in the electrophoretic analysis. The concentration of EtX and pEtX was 100nM. This figure is representative of the three independent experiments performed.

intercellular signaling.²⁷ Three main groups of EVs have been identified: exosomes, ectosomes, and apoptotic bodies.³⁹ Due to their size, exosomes, which are generated through an endo-exocytosis membrane cycle, were ruled out as the predominant population. Our experiments with caspase-3 also indicated that these vesicles were not predominantly apoptotic bodies. Finally, ectosomes, which are formed by the pinching off of the PM, are likely to be the vesicles observed. In this context, movie 2 supports this conclusion. However, more experimental work is required to establish the molecular and cellular nature of this EV population in accordance with the guidelines of the International Society for Extracellular Vesicles.³⁹

The MAL protein is the proposed receptor for EtX from *C. perfringens*.⁸ Our findings show that hMAL-expressing *Xenopus* oocytes release ATP similarly to several cell types that are sensitive to EtX^{9,16} and as observed with other PFTs.⁵¹ The high specificity of the effect of

EtX in *Xenopus* oocytes expressing hMAL was revealed by the fact that the expression of other unrelated proteins (such as Kir4.1 channels or aquaporin) did not make them responsive to EtX (Figures S9–S11). Although EtX is reported to subtly inhibit Kir channels in oligodendrocytes,⁵² our experiments showed no such activity.

It should be noted that human MAL, but not the endogenous MAL of *Xenopus* oocytes, supports the EtX-induced release of ATP. Based on the hydrophobic interaction and hydrogen bonds,⁵³ key amino acids in the largest isoform of MAL (P21145-1, UniProt) interact with EtX. It is not known whether EtX interacts with the other 3 isoforms of hMAL. It is of interest to understand how the interaction between MAL and EtX results in intracellular Ca²⁺ mobilization. Previous studies have suggested that Ca²⁺ is concentrated intracellularly inside the smooth ER of the ER-PM junctions.⁵⁴ MAL is found in lipid rafts,⁵³ where G protein-coupled receptors (GPCRs)

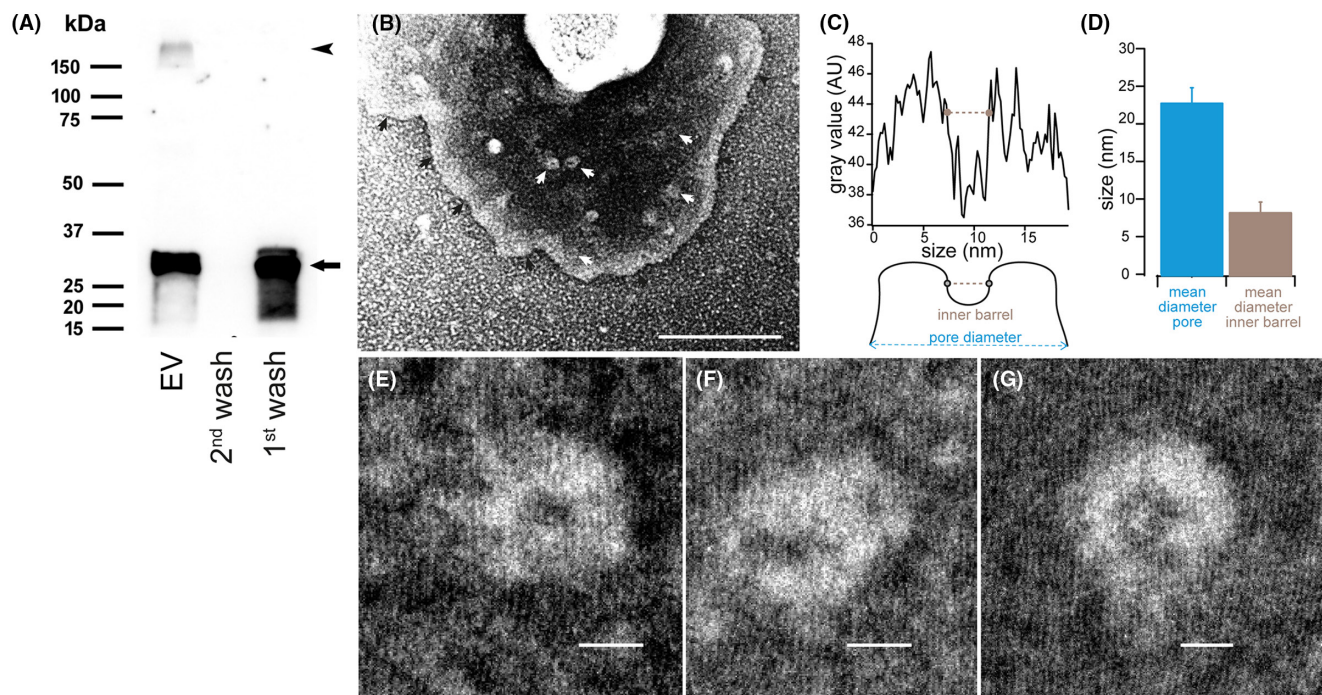


FIGURE 7 Etx oligomers in EVs. (A) Immunoblotting of EVs. Anti-Etx antibody was used to detect toxin molecules present in EV, which were collected after centrifuging the solution that contained hMAL oocytes exposed to Etx. Exposure to pEtx did not yield detectable amounts of EV. The first and second wash lanes correspond to the supernatant collected from the first and second centrifuges, before resuspension of the EV. Etx monomers were detected in the first supernatant but not in the second. After the second centrifugation Etx was detected in the sediment (EV lane). The arrow shows monomeric Etx and the arrowhead shows Etx oligomers. This experiment was repeated in four frogs and the most representative image is shown here. (B–G) In five experiments, we isolated EV from the bath medium after 30 min of exposure of hMAL oocytes to Etx (300 nM), and negative staining was performed. (B) An example of negative staining of an EV. Only part of the vesicle with a diameter larger than 600 nm is displayed. Black arrowheads indicate the limit of the membrane. Inside of this delimited region, diverse circular light structures, with a doughnut-like shape, are seen and some of them are labeled with white arrowheads (scale bar: 200 nm). (C) *Upper panel* shows the profile of the gray value (in arbitrary units (AU)) of one of the doughnut-like selected structures. We differentiate between the pore diameter (sky blue) and the inner barrel diameter (brown), which is represented in the *lower panel*. (D) Mean distance of the pore and inner barrel diameter ($N = 12$ selected structures). (E–G) Close-up of the distinctive structures (scale bar: 10 nm).

also occur. In sensory neurons, the activation of GPCRs by **bradykinin** mobilizes intracellular calcium by activating **IP3R** in the ER.⁵⁵ This type of local Ca^{2+} mobilization may funnel Ca^{2+} through the ER lumen to activate a spatially separate Ca^{2+} effector, which has been previously observed in *Xenopus* oocytes.⁵⁶ In a set of preliminary experiments, we explored whether the MAL-Etx complex can activate GPCRs. Oocytes were injected with **GDP- β -S**, a non-hydrolysable GDP analog, at an estimated final concentration of 1 mM. The objective was to permanently inhibit the **α -Gq** subunit, which is directly associated with IP3 generation. Among the four oocytes we used, we did not observe Etx-induced ATP release. However, we could not determine whether this lack of observation was due to an inhibitory effect or simply the death of the oocytes.

Lipid rafts also contain CaCCs/TMEM16, whose C-terminus interacts directly with the first intracellular loop of the IP3R. This interaction allows for direct Ca^{2+} mobilization.^{38,55,57,58} We examined the impact of **2-aminoethoxydiphenyl borate (2-APB)**, an antagonist of the IP3R, at a concentration of 100 micromolar for a duration of 30 min. Despite this treatment, Etx continued to induce ATP release and the extended incubation resulted in oocyte death,

as indicated by their morphology (data not shown). Further investigation is needed to understand how Etx, through its interaction with MAL, generates IP3, activates the IP3R, and induces Ca^{2+} release from the ER.

The increase in intracellular $[\text{Ca}^{2+}]$ induces the activation of CaCCs, which have been cloned in various cell types^(41,59,60), including *Xenopus* oocytes.^{36,41} CaCCs are also known as TMEM16A, ANO1, and DOG1. Etx-induced CaCC activation has been confirmed using MONNA, a potent TMEM16A blocker,³⁷ and TMEM16A antisense oligonucleotides (α -xTMEM16A). This activation depends on the presence of the MAL protein, as CaCC currents are inhibited by α -xMAL oligonucleotides. Our findings suggest that activated CaCCs may contribute to the reduction in the cellular and tissue resistance induced by Etx.^{61,62} CaCC currents in Etx-treated oocytes are driven by intracellular $[\text{Ca}^{2+}]$, although they can also respond to both $[\text{Ca}^{2+}]$ and voltage^(41,63).

CaCCs belong to the family of TMEM16 proteins that are phylogenetically derived from an ancestor with scramblase activity. The scramblase activity rapidly translocates phospholipids between the two leaflets of the membrane. It is Ca^{2+} -dependent and

does not require metabolic energy.⁶⁴ This activity is measured by the presence of PS, which is physiologically more concentrated at the inner leaflet, on the extracellular surface. The application of pSIVA demonstrated that Etx induced scramblase activity in the hMAL oocytes, leading us to speculate whether the hotspots of PS exposure colocalised with the ER-PM junctions. The PS extracellular exposure was further confirmed in an Etx-sensitive cell line (MOLT-4), which we also used to reveal that no apoptotic bodies were generated by Etx. Instead, the Etx action is intimately associated with the activation of a scramblase. TMEM16F is recognized as the protein that is critically involved in Ca²⁺-induced phospholipid scrambling in the PM. However, TMEM16F exhibits low expression in the PM of *Xenopus* oocytes⁴³ and does not adopt a unique conformation. Instead, its heterogeneous structure directly contributes to a variety of physiological functions.⁶⁵ In *Xenopus* oocytes, understanding the role of TMEM16F is challenging, as heterodimer formation between TMEM16F and TMEM16A is not feasible. However, TMEM16A may potentially engage in heterodimerisation with other TMEM16 proteins.⁶⁶ Due to the low levels of TMEM16F on the PM of *Xenopus* oocytes,⁴³ the origin of the Etx-induced scramblase activity is unknown. To explain our findings, we speculate that TMEM16A, which is highly expressed in the PM of *Xenopus* oocytes, may be involved in this activity. This speculation is based on the fact that TMEM16 proteins evolved from a common ancestor with scramblase activity, with TMEM16A and TMEM16B more recently acquiring anion channel functionality.⁶⁷ TMEM16A acts as an anion channel under physiological conditions. However, the introduction of a single amino acid mutation, such as L543K in murine TMEM16A⁶⁸ or V543T or V543S,⁶⁹ is sufficient to confer scramblase activity to TMEM16A. Notably, elegant experiments employing protein chimeras constructed from TMEM16A and TMEM16F have demonstrated the interchangeability of channel and scramblase activities between these proteins.⁷⁰ A plausible argument for the Etx-induced activity could be that TMEM16A, typically classified as a pure CaCC within the TMEM16 family, gains scramblase activity in the PM under the influence of hMAL and Etx. The results from the antisense oligonucleotide experiments in conjunction with those from the MONNA inhibition studies are in line with this hypothesis. In this context, other TMEM16 proteins exhibit a dual function involving both channel and scramblase activities, as observed with TMEM16F⁴⁴). Beyond these speculations, more research is needed to precisely identify the molecular nature of the scramblase activated by Etx.

Recent findings indicate that TMEM16F is activated by PFTs such as the *Listeria* toxin and the streptolysin O exotoxin.⁷¹ Similarly, we found that Etx induced the formation of EVs, with this process independent with respect to cell death by apoptosis. Vesicle formation relies on Ca²⁺-dependent TMEM16F activation in cell PMs.⁷² The formation of vesicles from the PM requires the bending and budding of the membrane, which occurs due to the redistribution of phospholipids between the two leaflets of the PM. This redistribution is facilitated by scramblases.

TMEM16F exhibits low expression in the PM of *Xenopus* oocytes.⁴³ The overexpression of TMEM16F in wild-type oocytes elicits only a limited ATP release, a hallmark of Etx activity, in the presence of the calcium ionophore A23187, which is approximately 25% of the ATP released from Etx-treated hMAL oocytes (Figure S8D,E). Despite these experiments linking vesicle formation to ATP release, the mechanism remains hypothetical, suggesting that ATP might escape during vesicle pinching-off via a fission pore akin to the endocytosis pore.⁷³ Notably, overexpressing TMEM16F alongside hMAL led to a decrease in the amount of ATP released instead of the expected increase in Etx-induced ATP release (Figure S8A,E). Western blots of EVs revealed Etx oligomers directly related to pore formation. Electron microscopy showed doughnut-like structures that are similar to the pores in cells exposed to PFTs.^{21,74} By contrast, the electrophysiological recordings did not indicate the formation of Etx pores in the PM. We therefore propose that Etx pores form in EVs, facilitating ATP release. Hence, our results suggest a dual ATP release mechanism: via membrane scission during vesicle formation and, more importantly, through Etx oligomer pores, explaining the delayed ATP release compared to the membrane capacitance decrease in the single-oocyte recordings. Further studies are required to determine whether EVs play a role in toxin elimination^{21,74} or contribute to the pathophysiology of PFTs. Additionally, our experimental findings indicate that Etx kills cells through a non-apoptotic pathway. Further research is needed to test whether Etx induces cell death through necrosis rather than apoptosis, as suggested by other studies.⁷⁵

In summary, we present a novel perspective on the mode of action of Etx, proposing a more intricate mechanism beyond the direct formation of PM pores in *Xenopus* oocytes. Our approach raises new questions, particularly regarding the potential role of EVs in the toxic effects of Etx.

AUTHOR CONTRIBUTIONS

Experiments were conceived by C.S. and J.B. M.C. and C.S. performed the experiments and analyzed the luminescence experiments. M.C. and C.S. performed the experiments and analyzed the two-electrode voltage-clamp data. S.R., M.C., and C.S. performed and analyzed the data on membrane capacitance. M.C., J.B., and J.D.A. performed the confocal microscopy for the calcium and scramblase activity and analyzed the results. M.B., M.M.S., and J.D.A. contributed to the development of the molecular tools used for cRNA synthesis and purification and oligonucleotide design. A.L. designed the electrophysiological analytical tools. M.C. and A.L. performed the light microscopy. M.C., B.T., and C.S. performed the electron microscopy. J.B. and J.D.A. performed the western blot analysis. M.C. and C.S. wrote the draft of the manuscript, which was revised by J.B. and J.D.A. All authors have read and approved the final manuscript.

ACKNOWLEDGMENTS

The authors thank Inmaculada Gómez de Aranda (Centres Científics i Tecnològics of the UB; CCiT) for technical assistance with the confocal and electron microscopy and flux cytometry.

The authors are also grateful to Professor Günther Schmalzing (RWTH Aachen University, Germany) for generously supplying the plasmids containing pNKs-mTMEM16A and pNKs-hTMEM16F for RNA synthesis, Dr Chris Patton (Stanford University, USA) for providing free access to the “Max-Chelator” software, and Professor John Dempster (Strathclyde University, Scotland, UK) for providing the “WinWCP” software for the electrophysiological studies. The authors thank the Language Service of the UB for the English revision of the manuscript. This study was supported by the Ministerio de Ciencia, Innovación y Universidades and the Agencia Estatal de Investigación (AEI) through grants SAF2017-85818-R and PID2021-126677NB-I00 funded by MCIN/AEI/10.13039/501100011033 and by the European Regional Development Fund (ERDF) “A way of making Europe.” We thank the CERCA (Centres de Recerca de Catalunya, SGR: 2021 SGR 01075) Programme/Generalitat de Catalunya for institutional support and the University of Barcelona for open-access financial support.

CONFLICT OF INTEREST STATEMENT

The authors declare no conflict of interest.

DATA AVAILABILITY STATEMENT

The data that support the findings of this study are available from the corresponding authors upon reasonable request.

ETHICS STATEMENT

Xenopus laevis specimens were handled in accordance with the guidelines approved by the local Catalan Government (reference 192/16, Animal Welfare Committee of the University of Barcelona).

ORCID

Mercè Cases  <https://orcid.org/0000-0003-2525-5475>

Jonatan Dorca-Arévalo  <https://orcid.org/0000-0001-7606-0462>

Marta Blanch  <https://orcid.org/0000-0003-1913-0158>

Sergi Rodil  <https://orcid.org/0000-0002-0277-6158>

Beatrice Terni  <https://orcid.org/0000-0001-9548-1625>

Mireia Martín-Satué  <https://orcid.org/0000-0002-9718-4664>

Artur Llobet  <https://orcid.org/0000-0001-5797-6782>

Juan Blasi  <https://orcid.org/0000-0002-0482-9444>

Carles Solsona  <https://orcid.org/0000-0002-9897-0667>

REFERENCES

- Dal Peraro M, van der Goot FG. Pore-forming toxins: ancient, but never really out of fashion. *Nat Rev Microbiol*. 2016;14(2):77-92. doi:10.1038/nrmicro.2015.3
- Podobnik M, Kisovec M, Anderluh G. Molecular mechanism of pore formation by aerolysin-like proteins. *Philos Trans R Soc Lond Ser B Biol Sci*. 2017;372(1726):20160209. doi:10.1098/rstb.2016.0209
- Cole AR, Gibert M, Popoff M, Moss DS, Titball RW, Basak AK. *Clostridium perfringens* epsilon-toxin shows structural similarity to the pore-forming toxin aerolysin. *Nat Struct Mol Biol*. 2004;11(8):797-798. doi:10.1038/nsmb804
- Savva CG, Clark AR, Naylor CE, et al. The pore structure of *Clostridium perfringens* epsilon toxin. *Nat Commun*. 2019;10(1):2641. doi:10.1038/s41467-019-10645-8
- Ma Y, Sannino D, Linden JR, et al. Epsilon toxin-producing *Clostridium perfringens* colonize the multiple sclerosis gut microbiome overcoming CNS immune privilege. *J Clin Invest*. 2023;133(9):e163239. doi:10.1172/JCI163239
- Rumah KR, Linden J, Fischetti VA, Vartanian T. Isolation of *Clostridium perfringens* type B in an individual at first clinical presentation of multiple sclerosis provides clues for environmental triggers of the disease. *PLoS One*. 2013;8(10):e76359. doi:10.1371/journal.pone.0076359
- Wagley S, Bokori-Brown M, Morcrette H, et al. Evidence of *Clostridium perfringens* epsilon toxin associated with multiple sclerosis. *Mult Scler*. 2019;25(5):653-660. doi:10.1177/1352458518767327
- Rumah KR, Ma Y, Linden JR, et al. The myelin and lymphocyte protein MAL is required for binding and activity of *Clostridium perfringens* epsilon-toxin. *PLoS Pathog*. 2015;11(5):e1004896. doi:10.1371/journal.ppat.1004896
- Blanch M, Dorca-Arévalo J, Not A, et al. The cytotoxicity of epsilon toxin from *Clostridium perfringens* on lymphocytes is mediated by MAL protein expression. *Mol Cell Biol*. 2018;38(19). doi:10.1128/MCB.00086-18
- Khalili S, Jahangiri A, Hashemi ZS, Khalesi B, Mard-Soltani M, Amani J. Structural pierce into molecular mechanism underlying *Clostridium perfringens* epsilon toxin function. *Toxicon*. 2017;127:90-99. doi:10.1016/j.toxicon.2017.01.010
- Linden JR, Flores C, Schmidt EF, et al. *Clostridium perfringens* epsilon toxin induces blood brain barrier permeability via caveolae-dependent transcytosis and requires expression of MAL. *PLoS Pathog*. 2019;15(11):e1008014. doi:10.1371/journal.ppat.1008014
- Linden JR, Ma Y, Zhao B, et al. *Clostridium perfringens* epsilon toxin causes selective death of mature oligodendrocytes and central nervous system demyelination. *MBio*. 2015;6(3):e02513. doi:10.1128/mBio.02513-14
- Dorca-Arévalo J, Dorca E, Torrejón-Escribano B, Blanch M, Martín-Satué M, Blasi J. Lung endothelial cells are sensitive to epsilon toxin from *Clostridium perfringens*. *Vet Res*. 2020;51(1):27. doi:10.1186/s13567-020-00748-2
- Geng Z, Kang L, Huang J, et al. Epsilon toxin from *Clostridium perfringens* induces toxic effects on skin tissues and HaCaT and human epidermal keratinocytes. *Toxicon*. 2021;198:102-110. doi:10.1016/j.toxicon.2021.05.002
- Morcrette H, Bokori-Brown M, Ong S, et al. Epsilon toxin vaccine candidate lacking toxicity to cells expressing myelin and lymphocyte protein. *NPJ Vaccines*. 2019;4:32. doi:10.1038/s41541-019-0128-2
- Chassin C, Bens M, de Barry J, et al. Pore-forming epsilon toxin causes membrane permeabilization and rapid ATP depletion-mediated cell death in renal collecting duct cells. *Am J Physiol Renal Physiol*. 2007;293(3):F927-F937. doi:10.1152/ajprenal.00199.2007
- Dorca-Arévalo J, Blanch M, Pradas M, Blasi J. Epsilon toxin from *Clostridium perfringens* induces cytotoxicity in FRT thyroid epithelial cells. *Anaerobe*. 2018;53:43-49. doi:10.1016/j.anaerobe.2018.05.011
- Dorca-Arévalo J, Gómez de Aranda I, Blasi J. New mutants of epsilon toxin from. *Toxins (Basel)*. 2022;14(4):288. doi:10.3390/toxins14040288
- Gaitán-Peñas H, Gradogna A, Laparra-Cuervo L, et al. Investigation of LRRc8-mediated volume-regulated anion currents in xenopus oocytes. *Biophys J*. 2016;111(7):1429-1443. doi:10.1016/j.bpj.2016.08.030
- Babychuk EB, Draeger A. Defying death: cellular survival strategies following plasmalemmal injury by bacterial toxins. *Semin Cell Dev Biol*. 2015;45:39-47. doi:10.1016/j.semcdb.2015.10.016
- Keyel PA, Loutcheva L, Roth R, et al. Streptolysin O clearance through sequestration into blebs that bud passively from the plasma

- membrane. *J Cell Sci.* 2011;124(Pt 14):2414-2423. doi:[10.1242/jcs.076182](https://doi.org/10.1242/jcs.076182)
22. Nagamune H, Ohnishi C, Katsuura A, et al. Intermedilysin, a novel cytotoxin specific for human cells secreted by *Streptococcus intermedius* UNS46 isolated from a human liver abscess. *Infect Immun.* 1996;64(8):3093-3100. doi:[10.1128/iai.64.8.3093-3100.1996](https://doi.org/10.1128/iai.64.8.3093-3100.1996)
 23. Donelli G, Fiorentini C, Matarrese P, et al. Evidence for cytoskeletal changes secondary to plasma membrane functional alterations in the in vitro cell response to *Clostridium perfringens* epsilon-toxin. *Comp Immunol Microbiol Infect Dis.* 2003;26(3):145-156. doi:[10.1016/s0147-9571\(02\)00052-8](https://doi.org/10.1016/s0147-9571(02)00052-8)
 24. Fernandez Miyakawa ME, Zabal O, Silberstein C. *Clostridium perfringens* epsilon toxin is cytotoxic for human renal tubular epithelial cells. *Hum Exp Toxicol.* 2011;30(4):275-282. doi:[10.1177/09603271110371700](https://doi.org/10.1177/09603271110371700)
 25. Petit L, Gibert M, Gillet D, Laurent-Winter C, Boquet P, Popoff MR. *Clostridium perfringens* epsilon-toxin acts on MDCK cells by forming a large membrane complex. *J Bacteriol.* 1997;179(20):6480-6487. doi:[10.1128/jb.179.20.6480-6487.1997](https://doi.org/10.1128/jb.179.20.6480-6487.1997)
 26. Popoff MR. Epsilon toxin: a fascinating pore-forming toxin. *FEBS J.* 2011;278(23):4602-4615. doi:[10.1111/j.1742-4658.2011.08145.x](https://doi.org/10.1111/j.1742-4658.2011.08145.x)
 27. Whitlock JM, Hartzell HC. Anoctamins/TMEM16 proteins: chloride channels flirting with lipids and extracellular vesicles. *Annu Rev Physiol.* 2017;79:119-143. doi:[10.1146/annurev-physiol-022516-034031](https://doi.org/10.1146/annurev-physiol-022516-034031)
 28. Curtis MJ, Alexander S, Cirino G, et al. Experimental design and analysis and their reporting II: updated and simplified guidance for authors and peer reviewers. *Br J Pharmacol.* 2018;175(7):987-993. doi:[10.1111/bph.14153](https://doi.org/10.1111/bph.14153)
 29. Harding SD, Sharman JL, Faccenda E, Southan C, et al. The IUPHAR/BPS guide to PHARMACOLOGY in 2018: updates and expansion to encompass the new guide to IMMUNOPHARMACOLOGY. *Nucleic Acids Res.* 2018;46(D1):D1091-D1106. doi:[10.1093/nar/gkx1121](https://doi.org/10.1093/nar/gkx1121)
 30. Alexander SPH, Christopoulos A, Davenport AP, et al. THE CONCISE GUIDE TO PHARMACOLOGY 2019/20: G protein-coupled receptors. *Br J Pharmacol.* 2019;176(Suppl 1):S21-S141. doi:[10.1111/bph.14748](https://doi.org/10.1111/bph.14748)
 31. Alexander SPH, Mathie A, Peters JA, et al. THE CONCISE GUIDE TO PHARMACOLOGY 2019/20: ion channels. *Br J Pharmacol.* 2019;176(Suppl 1):S142-S228. doi:[10.1111/bph.14749](https://doi.org/10.1111/bph.14749)
 32. Tanaka S, Endo H, Adegawa S, Kikuta S, Sato R. Functional characterization of bacillus thuringiensis cry toxin receptors explains resistance in insects. *FEBS J.* 2016;283(24):4474-4490. doi:[10.1111/febs.13952](https://doi.org/10.1111/febs.13952)
 33. Aleu J, Blasi J, Solsona C, Marsal J. Calcium-dependent acetylcholine release from xenopus oocytes: simultaneous ionic currents and acetylcholine release recordings. *Eur J Neurosci.* 2002;16(8):1442-1448. doi:[10.1046/j.1460-9568.2002.02208.x](https://doi.org/10.1046/j.1460-9568.2002.02208.x)
 34. Kuruma A, Hartzell HC. Dynamics of calcium regulation of chloride currents in xenopus oocytes. *Am J Phys.* 1999;276(1):C161-C175. doi:[10.1152/ajpcell.1999.276.1.C161](https://doi.org/10.1152/ajpcell.1999.276.1.C161)
 35. Kuruma A, Hartzell HC. Bimodal control of a Ca(2+)-activated Cl(-) channel by different Ca(2+) signals. *J Gen Physiol.* 2000;115(1):59-80. doi:[10.1085/jgp.115.1.59](https://doi.org/10.1085/jgp.115.1.59)
 36. Marin M. Calcium signaling in xenopus oocyte. *Adv Exp Med Biol.* 2012;740:1073-1094. doi:[10.1007/978-94-007-2888-2_49](https://doi.org/10.1007/978-94-007-2888-2_49)
 37. Oh SJ, Hwang SJ, Jung J, et al. MONNA, a potent and selective blocker for transmembrane protein with unknown function 16/anoctamin-1. *Mol Pharmacol.* 2013;84(5):726-735. doi:[10.1124/mol.113.087502](https://doi.org/10.1124/mol.113.087502)
 38. Cabrita I, Benedetto R, Fonseca A, et al. Differential effects of anoctamins on intracellular calcium signals. *FASEB J.* 2017;31(5):2123-2134. doi:[10.1096/fj.201600797RR](https://doi.org/10.1096/fj.201600797RR)
 39. Théry C, Witwer KW, Aikawa E, et al. Minimal information for studies of extracellular vesicles 2018 (MISEV2018): a position statement of the International Society for Extracellular Vesicles and update of the MISEV2014 guidelines. *J Extracell Vesicles.* 2018;7(1):1535750. doi:[10.1080/20013078.2018.1535750](https://doi.org/10.1080/20013078.2018.1535750)
 40. Falcieri E, Martelli AM, Bareggi R, Cataldi A, Cocco L. The protein kinase inhibitor staurosporine induces morphological changes typical of apoptosis in MOLT-4 cells without concomitant DNA fragmentation. *Biochem Biophys Res Commun.* 1993;193(1):19-25. doi:[10.1006/bbrc.1993.1584](https://doi.org/10.1006/bbrc.1993.1584)
 41. Schroeder BC, Cheng T, Jan YN, Jan LY. Expression cloning of TMEM16A as a calcium-activated chloride channel subunit. *Cell.* 2008;134(6):1019-1029. doi:[10.1016/j.cell.2008.09.003](https://doi.org/10.1016/j.cell.2008.09.003)
 42. Ousingsawat J, Wanitchakool P, Kmit A, et al. Anoctamin 6 mediates effects essential for innate immunity downstream of P2X7 receptors in macrophages. *Nat Commun.* 2015;6:6245. doi:[10.1038/ncomms7245](https://doi.org/10.1038/ncomms7245)
 43. Stolz M, Klapperstuck M, Kendzierski T, et al. Homodimeric anoctamin-1, but not homodimeric anoctamin-6, is activated by calcium increases mediated by the P2Y1 and P2X7 receptors. *Pflugers Arch.* 2015;467(10):2121-2140. doi:[10.1007/s00424-015-1687-3](https://doi.org/10.1007/s00424-015-1687-3)
 44. Yang H, Kim A, David T, et al. TMEM16F forms a Ca²⁺-activated cation channel required for lipid scrambling in platelets during blood coagulation. *Cell.* 2012;151(1):111-122. doi:[10.1016/j.cell.2012.07.036](https://doi.org/10.1016/j.cell.2012.07.036)
 45. Nguyen DM, Chen LS, Yu WP, Chen TY. Comparison of ion transport determinants between a TMEM16 chloride channel and phospholipid scramblase. *J Gen Physiol.* 2019;151(4):518-531. doi:[10.1085/jgp.201812270](https://doi.org/10.1085/jgp.201812270)
 46. Petit L, Maier E, Gibert M, Popoff MR, Benz R. *Clostridium perfringens* epsilon toxin induces a rapid change of cell membrane permeability to ions and forms channels in artificial lipid bilayers. *J Biol Chem.* 2001;276(19):15736-15740. doi:[10.1074/jbc.M010412200](https://doi.org/10.1074/jbc.M010412200)
 47. Azarashvili T, Odinkova I, Krestinina O, et al. Role of Phosphorylation of Porine proteins in regulation of mitochondrial outer membrane under Normal conditions and alcohol intoxication. *Biol Membr.* 2011;28(1):14-24.
 48. Beer KB, Wehman AM. Mechanisms and functions of extracellular vesicle release in vivo-what we can learn from flies and worms. *Cell Adhes Migr.* 2017;11(2):135-150. doi:[10.1080/19336918.2016.1236899](https://doi.org/10.1080/19336918.2016.1236899)
 49. Kalra H, Drummen GP, Mathivanan S. Focus on extracellular vesicles: introducing the next small big thing. *Int J Mol Sci.* 2016;17(2):170. doi:[10.3390/ijms17020170](https://doi.org/10.3390/ijms17020170)
 50. Karpman D, Ståhl AL, Arvidsson I. Extracellular vesicles in renal disease. *Nat Rev Nephrol.* 2017;13(9):545-562. doi:[10.1038/nrneph.2017.98](https://doi.org/10.1038/nrneph.2017.98)
 51. Lizak M, Yarovinsky TO. Phospholipid scramblase 1 mediates type I interferon-induced protection against staphylococcal α -toxin. *Cell Host Microbe.* 2012;11(1):70-80. doi:[10.1016/j.chom.2011.12.004](https://doi.org/10.1016/j.chom.2011.12.004)
 52. Bossu JL, Wioland L, Doussau F, Isope P, Popoff MR, Poulain B. Epsilon toxin from *Clostridium perfringens* causes inhibition of potassium inward rectifier (Kir) channels in oligodendrocytes. *Epsilon Toxin from Toxins (Basel).* 2020;12(1):36. doi:[10.3390/toxins12010036](https://doi.org/10.3390/toxins12010036)
 53. Lara-Lemus R. On the role of myelin and lymphocyte protein (MAL) in cancer: a puzzle with two faces. *J Cancer.* 2019;10(10):2312-2318. doi:[10.7150/jca.30376](https://doi.org/10.7150/jca.30376)
 54. Gardiner DM, Grey RD. Membrane junctions in xenopus eggs: their distribution suggests a role in calcium regulation. *J Cell Biol.* 1983;96(4):1159-1163. doi:[10.1083/jcb.96.4.1159](https://doi.org/10.1083/jcb.96.4.1159)
 55. Jin X, Shah S, Liu Y, et al. Activation of the Cl⁻ channel ANO1 by localized calcium signals in nociceptive sensory neurons requires coupling with the IP3 receptor. *Sci Signal.* 2013;6(290):ra73. doi:[10.1126/scisignal.2004184](https://doi.org/10.1126/scisignal.2004184)
 56. Courjaret R, Machaca K. Mid-range Ca²⁺ signalling mediated by functional coupling between store-operated Ca²⁺ entry and IP3-dependent Ca²⁺ release. *Nat Commun.* 2014;5:3916. doi:[10.1038/ncomms4916](https://doi.org/10.1038/ncomms4916)

57. Jin X, Shah S, Du X, Zhang H, Gamper N. Activation of Ca(2+)-activated Cl(-) channel ANO1 by localized Ca(2+) signals. *J Physiol*. 2016;594(1):19-30. doi:[10.1113/jphysiol.2014.275107](https://doi.org/10.1113/jphysiol.2014.275107)
58. Pacheco J, Ramirez-Jarquín JO, Vaca L. Microdomains associated to lipid rafts. *Adv Exp Med Biol*. 2016;898:353-378. doi:[10.1007/978-3-319-26974-0_15](https://doi.org/10.1007/978-3-319-26974-0_15)
59. Caputo A, Caci E, Ferrera L, et al. TMEM16A, a membrane protein associated with calcium-dependent chloride channel activity. *Science*. 2008;322(5901):590-594. doi:[10.1126/science.1163518](https://doi.org/10.1126/science.1163518)
60. Yang YD, Cho H, Koo JY, et al. TMEM16A confers receptor-activated calcium-dependent chloride conductance. *Nature*. 2008;455(7217):1210-1215. doi:[10.1038/nature07313](https://doi.org/10.1038/nature07313)
61. Cases M, Llobet A, Terni B, et al. Acute effect of pore-forming. *eNeuro*. 2017;4(4):ENEURO.0051-ENEURO17.2017. doi:[10.1523/ENEURO.0051-17.2017](https://doi.org/10.1523/ENEURO.0051-17.2017)
62. Wioland L, Dupont JL, Doussau F, et al. Epsilon toxin from *Clostridium perfringens* acts on oligodendrocytes without forming pores, and causes demyelination. *Cell Microbiol*. 2015;17(3):369-388. doi:[10.1111/cmi.12373](https://doi.org/10.1111/cmi.12373)
63. Le SC, Liang P, Lowry AJ, Yang H. Gating and regulatory mechanisms of TMEM16 ion channels and scramblases. *Front Physiol*. 2021;12:787773. doi:[10.3389/fphys.2021.787773](https://doi.org/10.3389/fphys.2021.787773)
64. Clarke RJ, Hossain KR, Cao K. Physiological roles of transverse lipid asymmetry of animal membranes. *Biochim Biophys Acta Biomembr*. 2020;1862(10):183382. doi:[10.1016/j.bbamem.2020.183382](https://doi.org/10.1016/j.bbamem.2020.183382)
65. Ye Z, Galvanetto N, Puppulin L, et al. Structural heterogeneity of the ion and lipid channel TMEM16F. *Nat Commun*. 2024;15(1):110. doi:[10.1038/s41467-023-44377-7](https://doi.org/10.1038/s41467-023-44377-7)
66. Tien J, Lee HY, Minor DL, Jan YN, Jan LY. Identification of a dimerization domain in the TMEM16A calcium-activated chloride channel (CaCC). *Proc Natl Acad Sci USA*. 2013;110(16):6352-6357. doi:[10.1073/pnas.1303672110](https://doi.org/10.1073/pnas.1303672110)
67. Kalienkova V, Clerico Mosina V, Paulino C. The groovy TMEM16 family: molecular mechanisms of lipid scrambling and ion conduction. *J Mol Biol*. 2021;433(16):166941. doi:[10.1016/j.jmb.2021.166941](https://doi.org/10.1016/j.jmb.2021.166941)
68. Le T, Jia Z, Le SC, Zhang Y, Chen J, Yang H. An inner activation gate controls TMEM16F phospholipid scrambling. *Nat Commun*. 2019;10(1):1846. doi:[10.1038/s41467-019-09778-7](https://doi.org/10.1038/s41467-019-09778-7)
69. Jiang T, Yu K, Hartzell HC, Tajkhorshid E. Lipids and ions traverse the membrane by the same physical pathway in the nhTMEM16 scramblase. *elife*. 2017;6:e28671. doi:[10.7554/eLife.28671](https://doi.org/10.7554/eLife.28671)
70. Schreiber R, Ousingsawat J, Wanitchakool P, et al. Regulation of TMEM16A/ANO1 and TMEM16F/ANO6 ion currents and phospholipid scrambling by Ca. *J Physiol*. 2018;596(2):217-229. doi:[10.1113/JP275175](https://doi.org/10.1113/JP275175)
71. Wu N, Cernysiov V, Davidson D, et al. Critical role of lipid scramblase TMEM16F in phosphatidylserine exposure and repair of plasma membrane after pore formation. *Cell Rep*. 2020;30(4):1129-1140. e1125. doi:[10.1016/j.celrep.2019.12.066](https://doi.org/10.1016/j.celrep.2019.12.066)
72. Han TW, Ye W, Bethel NP, et al. Chemically induced vesiculation as a platform for studying TMEM16F activity. *Proc Natl Acad Sci USA*. 2019;116(4):1309-1318. doi:[10.1073/pnas.1817498116](https://doi.org/10.1073/pnas.1817498116)
73. Cabeza JM, Acosta J, Alés E. Dynamics and regulation of endocytotic fission pores: role of calcium and dynamin. *Traffic*. 2010;11(12):1579-1590. doi:[10.1111/j.1600-0854.2010.01120.x](https://doi.org/10.1111/j.1600-0854.2010.01120.x)
74. Romero M, Keyel M, Shi G, et al. Intrinsic repair protects cells from pore-forming toxins by microvesicle shedding. *Cell Death Differ*. 2017;24(5):798-808. doi:[10.1038/cdd.2017.11](https://doi.org/10.1038/cdd.2017.11)
75. Ou L, Ye B, Sun M, et al. Mechanisms of intestinal epithelial cell damage by *Clostridium perfringens*. *Anaerobe*. 2024;87:102856. doi:[10.1016/j.anaerobe.2024.102856](https://doi.org/10.1016/j.anaerobe.2024.102856)

SUPPORTING INFORMATION

Additional supporting information can be found online in the Supporting Information section at the end of this article.

How to cite this article: Cases M, Dorca-Arévalo J, Blanch M, et al. The epsilon toxin from *Clostridium perfringens* stimulates calcium-activated chloride channels, generating extracellular vesicles in *Xenopus* oocytes. *Pharmacol Res Perspect*. 2024;12:e70005. doi:[10.1002/prp2.70005](https://doi.org/10.1002/prp2.70005)